An Apparatus to Determine the Pull-Off Force of a Conducting Microparticle from a Charged Surface

T. R. Szarek and P. F. Dunn

Particle Dynamics Laboratory, Department of Aerospace and Mechanical Engineering, University of Notre Dame, Notre Dame, Indiana, USA

A unique experimental apparatus has been developed to determine the pull-off force of a conducting microparticle resting on a conducting surface in the presence of a DC electric field. The apparatus precisely measures the applied electric-field strength at which an individual microparticle of known diameter, which is measured *in situ*, is removed from the surface. This information is used to determine the adhesion pull-off force required to remove the microparticle from the surface to within an uncertainty of approximately 12% at 95% confidence. In the experiment, the electric field strength between a conducting-surface electrode and a grounded electrode is increased in time using a microcontroller-driven digital-to-analog converter. Both electrodes are semi-transparent, which permits the surface-resident microparticles to be viewed from underneath the surface using microphotography. The microphotography system is operated in conjunction with pixel-intensity, gradient-search software to determine the diameter of each surface-resident microparticle. The apparatus is designed to explore a wide range of operating conditions, including microparticles of diverse composition and sizes, surfaces of differing roughness, and environments of various relative humidity including vacuum. The theory of operation and instrument design are presented in detail. Preliminary results also are given as a proof of concept.

INTRODUCTION

An electrostatic particle dispenser (EPD) is a device that consists of two or more conducting plates between which the microparticles to be dispensed are placed. When an electric field of sufficient intensity is established between these plates, the microparticles become charged, attracted to the oppositely charged plate, and proceed to bounce between the plates until they exit at a specific speed through an orifice located in one of the plates.

References to using electrostatics to dispense conducting microparticles can be found as early as 1960. Shelton, Hendricks,

and Wuerker (1960) developed a device to accelerate microparticles to hypervelocities (as high as 3 km/s) using very intense electric fields. Later, Adamo and Nanevicz (1975) developed a system to dispense microparticles in a vacuum at a regular and controllable rate. A device similar to that developed by Adamo and Nanevicz was used by Caylor, Dunn, and Brach (1993) in a study of microparticle impact on surfaces.

The operation of an EPD ultimately is limited by the breakdown voltage of the gas between its two conducting plates. For small particles, where particle-surface adhesion is more dominant, it may not be possible to achieve an electric field strength that is large enough to levitate the particles from the surface. Because it may not be possible to control the environmental operating conditions of the EPD, a detailed understanding of the particle-surface adhesion force in the dispenser under a variety of conditions is required to completely define the dispenser's operational range.

The first proposed use of an EPD to study adhesion was made by Myazdriker and Pusanov (1969). The system consisted of two parallel electrodes onto which microparticles were placed. The lower electrode was made of iridium-treated glass that served as a transparent conductor. This allowed the particles to be illuminated from behind and viewed with a microscope. The upper electrode was a fine-metal gauze. The instrument was operated with air between the plates. In order to delay voltage breakdown between the electrodes, the air pressure between the plates was increased. The inability to observe a large number of particles in real time precluded obtaining a statistically significant sample of data. Only general trends in the data were published.

Cho (1964) measured the charge on conducting particles exiting from an EPD, confirming the theoretical relationship between applied electric field and particle charging. Adhesion was not directly investigated. Subsequently, Colver (1976) studied the charge on both conducting and dielectric particles. In his study, the charge of the particles was determined based on the applied voltage level when the particles left the surface. However, in order to avoid complications associated with an adhesion force, larger particles, on the order of several hundred micrometers in diameter, were used. This resulted in the gravitational force being much larger than the adhesion force.

Copper, Wolfe, and Miller (1988) made the first practical study of particle adhesion in the presence of an electric field. Particles resting on a highly polished, conductive surface were exposed to an electric field of known magnitude for five minutes under high-vacuum conditions. The difference between the number of particles observed before and after the experiment characterized the removal efficiency. Following this lead, Olansen, Dunn, and Novick (1989) investigated the operational limits of an EPD under both atmospheric and vacuum conditions. Their study focused on layers of particles rather than individual particles dispensed on the conducting surface. This introduced the effect of inter-particle cohesion in addition to particle-electrode surface adhesion on the dispensing rate of the particles (Novick, Hummer, and Dunn 1989).

To achieve a more detailed understanding of microparticle adhesion in an EPD, a unique measurement system has been developed to determine the adhesion force for microparticles of known size and composition in the presence of an electric field. This system can operate under various humidity and pressure conditions and include surfaces with differing roughness profiles. It can be used for detailed measurements of adhesion forces of individual particles.

BACKGROUND

A microparticle resting on a surface inside an EPD is acted upon by gravitational, F_g, electrostatic, F_e, adhesion F_a, and compression (Hertzian), F_H, forces. The two surface-contact forces, F_H and F_a, usually are combined and referred to as the "adhesion" force, or here, the total force of adhesion, F_{adh}, as depicted in Figure 1. The total force of adhesion is the net force at static equilibrium that holds the microparticle on the surface. As the microparticle is being removed from the surface by an increasing upward force, the microparticle continues to remain attached to the surface until it snaps off of the surface. The adhesion force when snap-off occurs, which is different than the total force of adhesion, is termed the pull-off force, F_{po}.

At the moment of snap-off, a particle being removed by an electric field is being acted upon by three forces: gravity, F_g, electrostatic, F_e, and adhesion, F_{adh}, which equals F_{po}. The gravitational force acts to keep the particle on the surface and can be calculated provided the plate's orientation (assumed perpendicular to gravity) and the particle's diameter and density are known, as described by the equation:

$$F_g = \rho \frac{\pi d^3}{6} g \qquad [1]$$

in which g represents the local gravitational acceleration, ρ the particle density, and d the particle diameter.

The electrostatic force acts to remove the particle from the surface. It results from the repulsion between the electrons transferred from the surface to the conducting particle's surface and the electrons on the surface local to the particle. A theoretical model for the charge of a spherical particle as a function of the
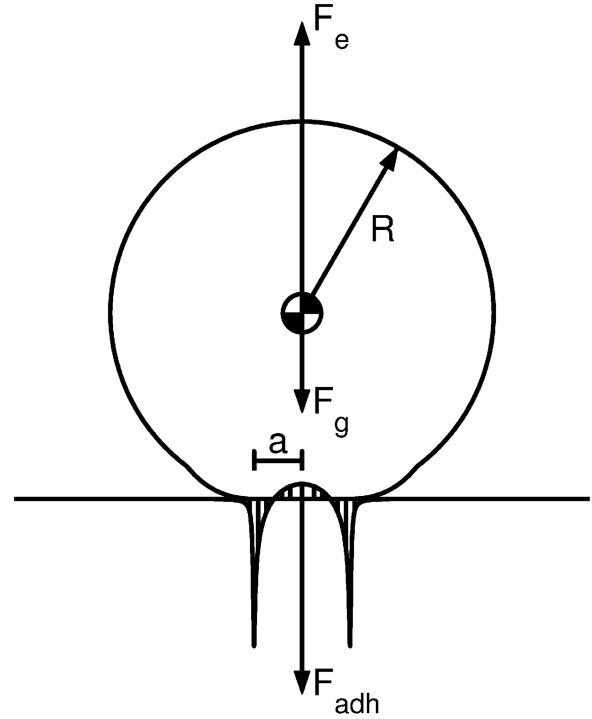

FIG. 1. Forces acting on a microsphere resting on a surface in the presence of an electric field where R is the particle radius, a the contact radius, F_e the electrostatic force acting on the particle, F_g the gravitational force, and F_{adh} the adhesion force, which is the sum of the Hertzian and adhesive forces. At the moment of detachment, $F_{adh} = F_{po}$ and is termed the pull-off force.

electric field has been verified experimentally by Cho (1964) and Colver (1976). This charge is:

$$q = \frac{\pi^2}{6} \varepsilon_0 \pi d^2 E_u = 1.64 \varepsilon_0 \pi d^2 E_u \qquad [2]$$

in which q is the particle charge, ε_0 the permittivity of free space, and E_u the intensity of the uniform electric field between the two parallel plates in the absence of the influence of the particle ($E_u = V/h$, in which V is the applied potential difference between the electrodes, and h the electrode spacing).

The electrostatic force is simply:

$$F_e = q E_l \qquad [3]$$

in which E_l is the intensity of local electric field, which equals $0.84\, E_u$ because of the presence of the particle (Myazdriker and Pusanov 1969).

The total force of adhesion acts with gravity to keep the particle on the surface. Its magnitude is the objective of this investigation. While it is possible that the total force of adhesion differs in magnitude between the electrically charged and electrically neutral cases, it is reasonable to assume that the parameters that affect the total force of adhesion of electrically neutral particles resting on electrically neutral surfaces may also apply to charged

particles resting on a surface having similar charge. The total force of adhesion for such particles at pull-off is assumed to be of the form:

$$F_{po} = C_1 \pi \gamma d (1 + C_2 RH) C_3 \qquad [4]$$

in which γ is the combined surface energy of adhesion and RH the relative humidity in percent. C_1 is a theoretical coefficient whose value is specified by Maugis (1991) to be between 0.75 and 1, the limits of the theories presented by Johnson, Kendal, and Roberts (1971) and Derjaguin, Muller, and Toporov (1975), respectively, as dictated by Tabor's parameter. Tabor's parameter can be interpreted as the ratio of the elastic displacement of the particle's surface at the point of separation from the substrate surface to the equilibrium atomic spacing. Low values of Tabor's parameter represent small, hard (non-compliant) particles, whereas large values represent large, soft (compliant) particles. C_2 is a coefficient that encompasses the effect of relative humidity. C_3 is the pull-off force reduction factor derived by Cheng, Dunn, and Brach (2002) that accounts for the effect of the asperity roughness height, that is, the surface roughness between the particle and electrode surface. C_1 and C_3 are dimensionless and are determined theoretically. C_2 also is dimensionless but is determined empirically.

The coefficient C_2 determines the increase in the adhesion force with increasing humidity. Experimental studies have shown that at moderate humidities, between 30% and 70%, the adhesion force increases linearly with relative humidity. A typical value for C_2 is 0.009, as given by Corn (1961). It should be noted that his study was conducted for specific particle compositions and the effect of surface roughness was not studied.

Finally, the coefficient C_3 accounts for a reduction in the pull-off force that results from surface asperities. Because the van der Waals attractive force between molecules decays as $1/z^6$ over short distances, where z is the separation distance between molecules, even small separation distances forced by these asperities will greatly reduce adhesion force. This reduction factor, determined from theory (Cheng, Dunn, and Brach 2002), is shown in Figure 2 as a function of the standard deviation of asperity heights. Note that for standard deviations as small as 2.0 nm, the reduction factor is 0.01, which is a 99% reduction in the theoretical adhesion force for a sphere on a perfectly flat surface. The magnitude of this reduction factor has been confirmed by experiments conducted by Ibrahim, Dunn, and Brach (2003).

In order to thoroughly study the factors affecting adhesion experimentally, particle size and composition are determined, while environmental conditions such as relative humidity, pressure, and temperature are either controlled or monitored. Additionally, several electrode surfaces with varying roughness profiles are utilized to study surface roughness effects on adhesion.

While both gravity and adhesion are constant for constant operating conditions, the electrostatic force will vary with the electric-field intensity. Therefore, when a sufficient electric field
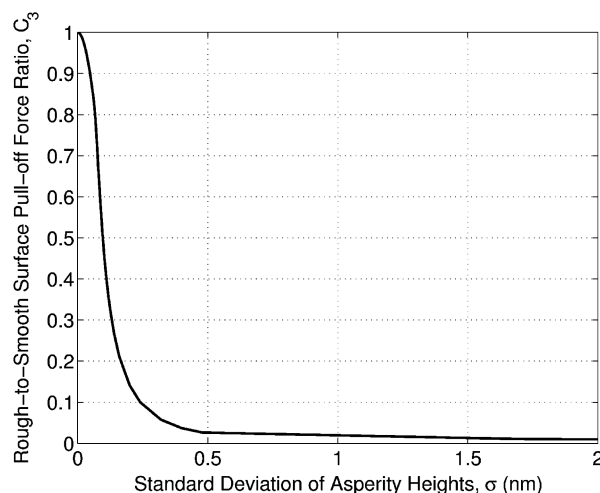

FIG. 2. Reduction factor of particle pull-off force, C_3, with increasing surface roughness as characterized by the standard deviation of surface asperity heights σ [from Cheng, Dunn, and Brach (2002)].

exists such that the electrostatic force exceeds the combined force of gravity and adhesion, the particle will leave the electrode and move to the oppositely charged electrode. This allows for a technique to determine the adhesion force for an individual particle when the magnitudes of both the gravitational and electrostatic forces are known at the moment of detachment. Thus, implementing such a technique requires that the particle's size be known, as well as the electric-field intensity at the moment of detachment.

INSTRUMENT DESIGN

This experimental system allows for the determination of the microparticle pull-off force by allowing for either control or monitoring of all the factors affecting that force. This includes the direct measurement of the diameter for individual microparticles. By operating in a vacuum chamber, environmental factors such a relative humidity, pressure, and temperature can be controlled. The effect of surface roughness is investigated by using several base surfaces with varying surface roughness profiles. Finally, the electric field is precisely controlled as a function of time, such that by observing when a particular particle is removed from the surface, the electric field required to do so is known. The entire setup is shown in Figure 3.

Two translucent but electrically conducting parallel electrodes are held a fixed distance apart. Particles are dispensed on the lower electrode. A microcontroller is programmed to deliver a known and repeatable voltage profile from a DC high-voltage supply. By slowly increasing the voltage difference between the plates, the electric field intensity rises until the electrostatic force exceeds the combined effect of gravity and adhesion, and the particle leaves the surface. A CCD camera mounted below the bottom plate monitors when a particular particle has left the surface.
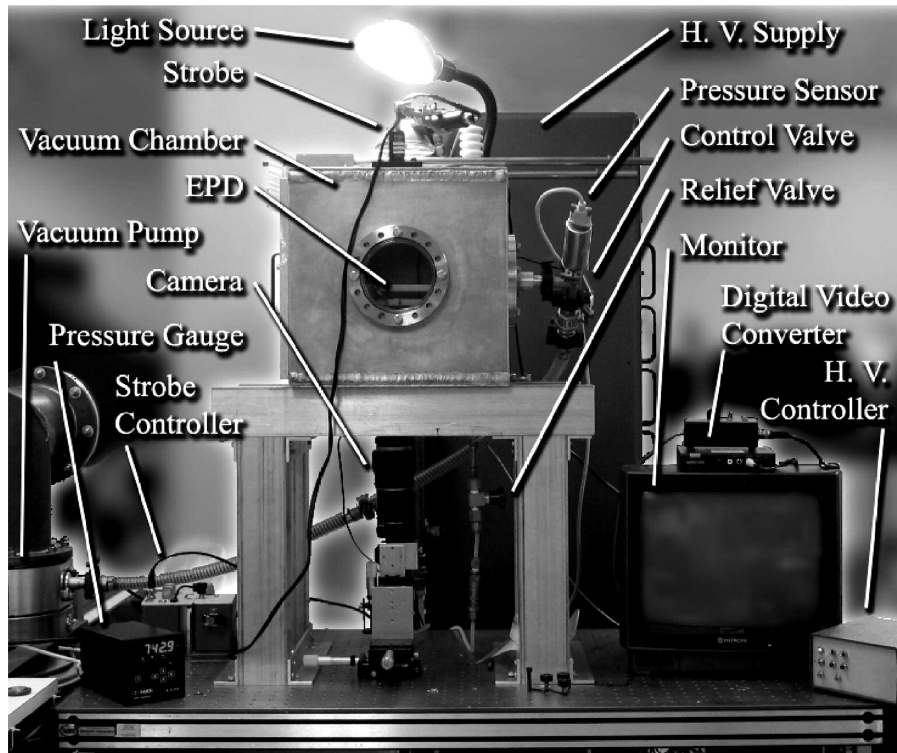
FIG. 3. Picture of experimental setup showing the EPD mounted inside the vacuum chamber, devices associated with the system operation, and instruments used for system monitoring and data collection.

The top electrode is a 10-cm diameter, metal-coated Petri dish. This dish, in addition to the obvious benefit of being clear, has the ideal shape for electrodes. Its flat underside allows for the creation of a uniform electric field while the rounded transition to the sides minimizes sparking. Initially, the bottom and sides of the Petri dishes were coated with a thin layer of aluminum approximately 200-nm thick using a Emitech $675\times$ DC sputterer. This allowed the surface to be conducting while still translucent; however, the aluminum was found to oxidize over time, so later experiments used gold-plated surfaces, as described in the following section.

At first, Petri dishes were used for both the upper and lower surfaces (all data presented herein used an aluminum-coated Petri dish as the substrate). However, in order to study the effect of varying surface roughness, three sets of 1-in. diameter glass optical flats were similarly treated. Each glass surface has differing initial surface roughness profile as characterized by the glass's optical quality. The glass flats are mounted inside a piece of aluminum machined to match the shape of the Petri dish. A thin annulus of aluminum makes contact with the outer edge of the coated surface, thus allowing the surface to become charged. The thickness of the contact is 0.3 mm and accounts for less than a 3% error in the uniform electric field over more than 75% of the surface.

For further studies, not reported herein, the surfaces were coated in gold to avoid the surface oxidation that occurs with aluminum. Gold not only is highly resistant to oxidation, but its surface energy has been well documented. This reduces the uncertainty associated with that term in the adhesion equation. Gold also does not react with nitric acid, allowing standard surface preparation techniques, as described in Phares, Smedley, and Flagan (2000), to be employed. A 50-nm layer of titanium is deposited first to aid in the bonding of the gold to the glass. A 200-nm layer of gold then is placed over the titanium using an FC-1800 electron-beam vacuum deposition/coating system.

Two supporting pieces made of Delrin®, a dielectric, are used to hold the surfaces parallel to one another at a fixed distance. The separation distance can be changed by sliding the top support piece along a track. The standard separation distance is 1 cm. The high-voltage supply lines are connected to the plate through a ball contact on the side of the Petri dishes, ensuring that the minimum distance between the two electrodes is between the plate surfaces, which minimizes sparking. The geometry is shown in Figure 4. A computational model verified the uniformity of the electric field over the surface of the plates for various spacings as shown in Figure 5.

The DC high-voltage source is generated by a Glassman PH Series High-Voltage DC power supply. The system transforms a 120-V wall supply into as much as 3 kW of energy with either a maximum voltage of 50 kV or a maximum current of 60 mA. Maximum ripple on the output is 0.25%. The voltage output is controlled via an analog input line.
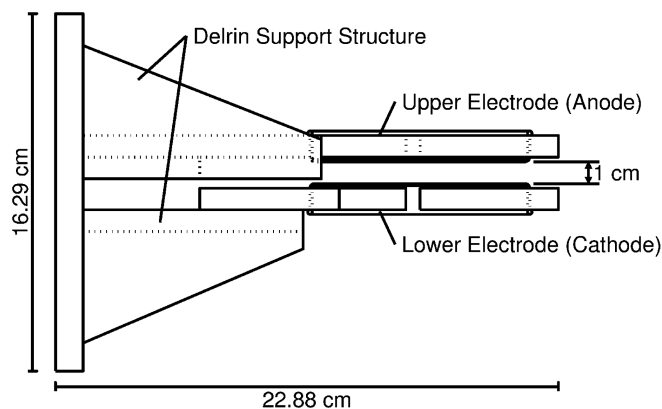
FIG. 4. Side schematic of electrode plates and support structure. The minimum distance between electrodes (plate surfaces) is 1 cm. The support structure is insulating Delrin®.

The voltage signal is generated using a digital-to-analog converter (DAC) controlled by a microcontroller. The Silicon Laboratories 8051F020 microcontroller is an 8051-derivative microcontroller with timer, interrupt, and digital I/O functionality. It also has eight on-board 12-bit A/D channels and two 12-bit DACs. One of these DACs is used to provide the voltage control for the high-voltage supply. The maximum output from this DAC is 2.43 V, the reference voltage for the chip's analog system, which provides a maximum high-voltage output of 12 kV.

An Astrovid 2000 Astronomical CCD video camera is mounted on a three-axis linear traverse below the plates. Several lenses are used to achieve the level of magnification required to see the particles, including an 80-mm lens, a telescopic converter, and, depending on the size of the particles being viewed, either a 2× or 3× magnification adapter or both at once for a 6× additional zoom. The analog signal from the CCD camera is converted to a digital one that is captured by a notebook
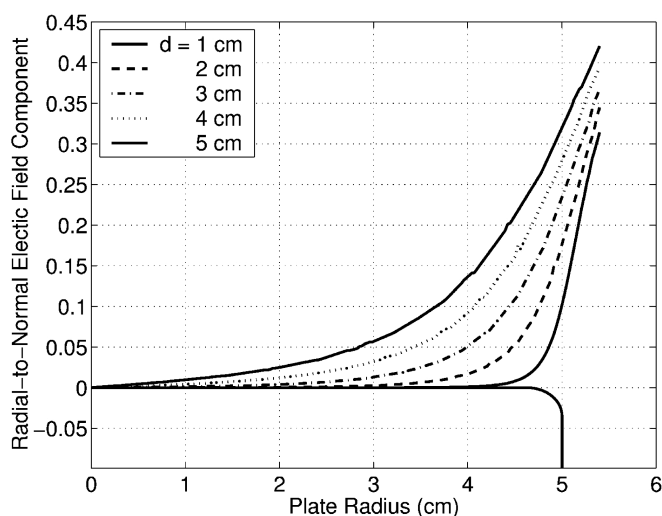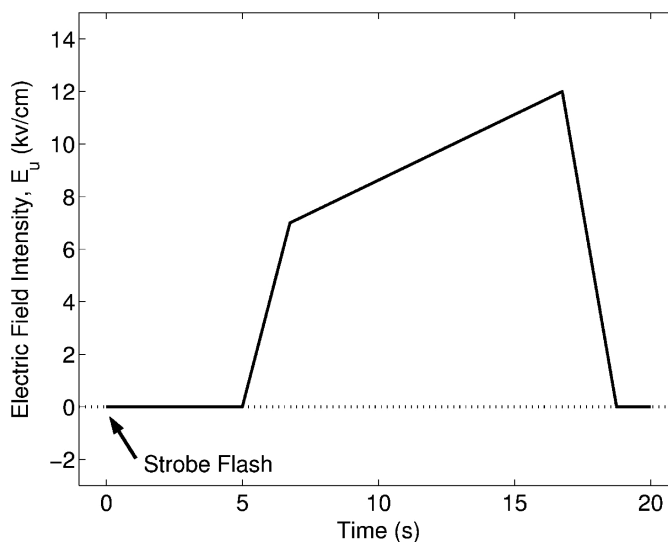
FIG. 6. A typical voltage profile including: a 5-s delay for strobe removal, a quick rise to the minimum expected levitation voltage, a slow rise in the region of interest, and finally discharge.

PC. A Canopus ADVC100 converts the video image in real time to a 640-by-480 pixel digital video with a frame rate of 30 frames/s. The typical resolution for the 6×-zoom configuration is 3.5 μm/pixel.

A strobe light is positioned in the field of view of the camera and is triggered at the start of the voltage profile to synchronize the video capture with the voltage supply. A typical voltage profile is shown in Figure 6. A short delay allows for the removal of the strobe light. The voltage then quickly rises to the minimum voltage level expected for levitation. A slow increase over the region of interest allows for the maximum temporal resolution. Once the maximum voltage of interest has been reached, the level is returned to zero.

Three different compositions of microparticles were used for the preliminary results reported herein. These were silver-coated glass, stainless steel, and nickel. The surface, as described previously, was aluminum coated.

While the present setup was developed independently, a similar system was proposed by Myazdriker and Pusanov (1969) using iridium-treated glass as mentioned earlier. In their setup, the pressure between the plates was increased to delay sparking. The present device is mounted in a vacuum chamber allowing for operation under vacuum condition where not only is sparking delayed, but also the effect of relative humidity is eliminated, thereby allowing baseline measurements to the taken for "dry" (zero relative humidity) conditions.

UNCERTAINTY ANALYSIS

Standard measurement uncertainty analysis (e.g., see Dunn 2005) can be applied to determine the uncertainty in an estimate of the pull-off force. This uncertainty results from those uncertainties in the direct measurements of other quantities (d,

FIG. 5. Calculated ratio of radial component of electric field to normal, electric-field component for various plate spacings.

TABLE 1
Uncertainties in measured and assumed quantities and in the forces dependent on these quantities.

Measurement/Result	Symbol	Value	Uncertainty	% Uncertainty
Particle Diameter (μm)	d	44.7	1.5	3.36
Plate Spacing (cm)	h	1.0	0.05	5.00
Removal Voltage (kV)	V	7.34	0.020	0.27
Electric Field (kV/m)	$E_u = V/h$	734	36.8	5.01
Particle Density (kg/m^3)	ρ	850	61.6	7.25
Electrostatic Force (nN)	F_e (Eq. 3)	41.2	4.97	12.1
Gravitational Force (nN)	F_g (Eq. 1)	0.39	0.05	12.4
Pull-off Force (nN)	$F_{po} = F_e - F_g$	40.8	4.97	12.2

h, and V), from a property (ρ), and from physical constants (ε_0 and g). For this experiment, the uncertainties in the physical constants are assumed negligible with respect to those in the other variables. Also, the error in the magnitude of the particle's charge is assumed negligible because of how well experiments (Cho 1964; Colver 1976) have confirmed Equation (2) for near-spherical, conducting particles, such as those which this study uses exclusively. Using this approach, the uncertainty in a single measurement of the pull-off force is estimated to be ±12.2% at 95% confidence.

The uncertainties for all of the quantities involved in determining the pull-off force uncertainty are presented in Table 1. The two largest sources of elemental uncertainty are the particle diameter and the plate spacing. Factors contributing to the uncertainty in the voltage when a particle is determined to leave the surface are a manufacturer-specified 0.25% maximum ripple, the resolution of the 12-bit digital-to-analog converter driving the high-voltage supply, and the temporal resolution of the video camera used to determine when a particle leaves the surface. The uncertainty in the plate spacing is assumed to be 5%, although care is taken to ensure the plate spacing is as close to 1 cm as possible, making this estimate conservative.

Because the calculation of the electrostatic force (see Equations [2] and [3]) requires knowledge of the particle diameter, the diameter must be determined in an accurate and repeatable manner. To do so, a particle-sizing algorithm was developed utilizing the video capture of the particles during removal.

The algorithm assumes that the particle's edge is the point of highest gradient when traveling outwards from the particle's center. This technique is more effective than an intensity method because it is relatively unaffected by lighting conditions, which can vary greatly between experiments and even in different regions of the surface during the same experiment. The algorithm is executed by a linearized best-fit of a locus of points that are determined to represent the particle's edge. The gradient along a series of 128 radials emanating from near the particle's center are evaluated and the maximum determined. A circle then is fit to those points with the x and y center location and the particle radius as parameters as shown in Figure 7. Only 16 of the 128 radials are shown in the figure for clarity.

To test the method, particles of well-defined size were examined. The routine was found to accurately measure the diameter of glass particles with mean diameters of 30 μm, 50 μm, and 70 μm under various zoom and lighting conditions. The mean particles sizes were determined to within the accuracy specified for the particles, typically with a bias of 1 μm larger than the expected mean. The standard deviations matched the specified standard deviations to within 20%. Accounting for the suspected bias and random error determined in the application of the algorithm, the uncertainty in the particle diameter is 1.5 μm.

RESULTS

Preliminary studies were conducted using this apparatus to verify the experimental setup and to explore the effects of microparticle size and composition as well as relative humidity on the microparticle pull-off force.
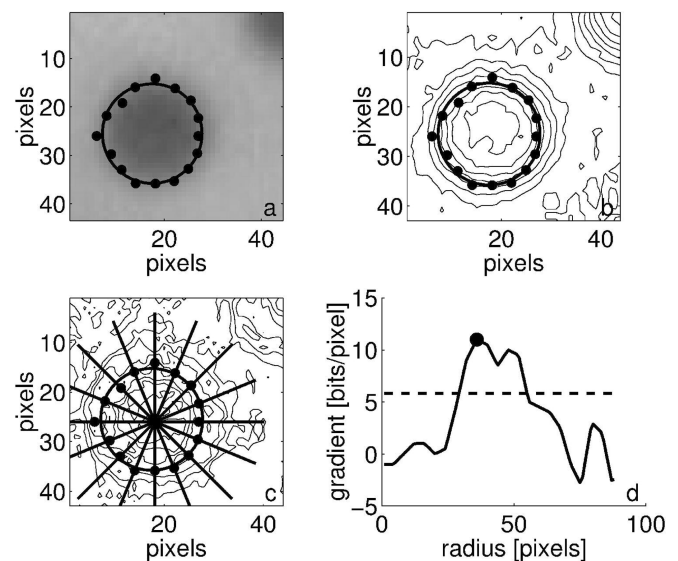

FIG. 7. Sizing algorithm routine applied to a typical particle showing: (a) the original video still with particle edge points and best-fit superimposed, (b) intensity contours, (c) gradient contours with 16 radials, and (d) gradient value along a typical radial with the maximum value marked.
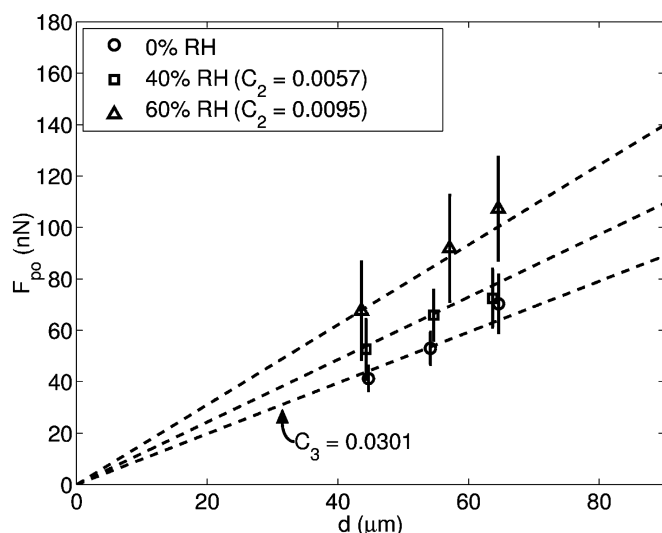
FIG. 8. Effect of relative humidity on pull-off force for silver-coated glass particles of various sizes. C1 is calculated to be 0.85. Υ is assumed to be 0.016 J/m^2. The 0% relative humidity case is the result of exposing the particles and surface to a vacuum with a pressure lower than the vapor pressure for water for 30 minutes.
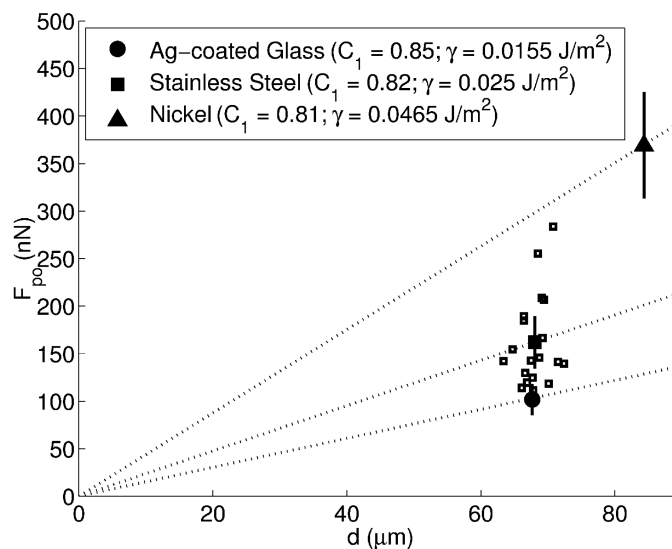

FIG. 9. Effect of microparticle composition on pull-off force for particles of similar size composed of silver-coated glass, stainless steel, and nickel. For each case, the relative humidity was 40%. From previous experiments, C_2 is 0.0057 and C_3 is 0.0301. Individual measurements are shown for stainless steel (open squares) as well as the averaged force measurement to show the degree of scatter observed in the data.

As expected (see Equation [4]), the determined mean adhesion force varied linearly with particle size, as shown in Figure 8. In this experiment, silver-coated glass particles of various sizes were studied at three relative humidities. Zero relative humidity was achieved by evacuating the experimental chamber to a pressure below the vapor pressure of water for 30 minutes and then introducing dry nitrogen to the chamber. From this data, values for C_2, which encompasses the effect of humidity, and C_3, the surface roughness reduction factor, could be estimated.

Using a calculated value for C_1 of 0.86 and an estimated value of γ of 0.016 J/m^2, which is explained in further detail below, the surface roughness reduction factor C_3 is 0.0301. This corresponds to a standard deviation of surface asperities of 0.45 nm. Preliminary surface profile measurements show that the most probable value for the standard deviation of surface asperities is less than 1.0 nm. More precise measurements are required to accurately determine smaller values.

The experiment also verifies an increase in adhesion with increasing relative humidity, as described by Equation 4. The ratio of the slope between the zero-humidity case and the 40% humidity case yields a value for C_2 of 0.0057. The value for 60% humidity is 0.0095. These values correspond well with previous experiments, such as those of Corn (1961), who determined a value for C_2 of 0.009. A lower value for the 40% humidity case is expected because it is near the region below which the relative humidity has no effect on adhesion. Ibrahim, Dunn, and Brach (2004) as well as others have shown that microparticle adhesion begins to increase from a constant value with increasing relative humidity at approximately 30% and then becomes relatively constant again at approximately 70%. Scatter in the data, shown by the error bars, is attributed to slight non-uniformities in the surface and to minor variations in the relative humidity local

to each microparticle. This scatter is observed to increase with increasing relative humidity.

The experiments further showed variation in the adhesion force for different materials. Silver-coated glass (P. A. Industries SF-44, 10 μm to 90 μm, sifted between 53 μm and 90 μm, 850 kg/m^3), stainless steel (Duke Scientific 451, 64 μm to 76 μm, 8000 kg/m^3), and nickel (Duke Scientific 358, 75 μm to 90 μm, 8900 kg/m^3) particles of similar size were tested under identical environmental and surface-roughness conditions. Noticeable differences in the adhesion force were observed, as shown in Figure 9. The value of C_2 was taken to be 0.0057 to correspond with 40 % relative humidity. The value of C_3 was taken to be 0.0301, as determined in the previous experiment. The value of C_1 was calculated for each material, but was relatively constant (between 0.81 and 0.85).

Using these values, the surface energy, γ, for each of the three material cases could be calculated as interacting with aluminum oxide, the assumed electrode surface composition. Table 2 shows the published surface energy values and the

TABLE 2
Comparison of published and determined surface-energy values.

Material[1]	Published[2]	Determined
Ag-coated Glass	0.016 J/m^2	0.015 J/m^2
Stainless Steel	0.036 J/m^2	0.025 J/m^2
Nickel	0.039 J/m^2	0.047 J/m^2

[1]Calculated interacting with aluminum-oxide.
[2]Osborne-Lee (1988) and Visser (1972).

empirically determined surface energy values. The determined values increase from silver-coated glass to stainless steel to nickel, as do the reported values.

The published values for γ were taken from various sources (Osborne-Lee 1988; Visser 1972), where the surface energy values were specified as Hamaker constants. Statistical variation between the sources and uncertainty introduced with the conversion to surface energy gives uncertainties of approximately 11.6% for stainless steel and nickel and 33.9% for silver-coated glass at 95% confidence.

The increased uncertainty in the silver-coated glass surface energy is the result on an assumption made in the calculation of the surface energy. Specified surface energies for silver on aluminum oxide result in a surface energy of 0.0465 J/m^2, larger than either stainless-steel or nickel. If, however, the silver coating on the particle is thin enough, then rather than treating the surface interaction as simply that between silver and aluminum oxide, it instead can be treated as that between glass and aluminum oxide with a silver medium. Under those circumstances, the determined surface energy value corresponds well with the measured value. The determined values agree to within less than 30%, which is within the combined uncertainty of the experimental uncertainty and reported uncertainties in published values. Further experimentation is required to more accurately determine all measured quantities.

SUMMARY AND CONCLUSIONS

An experimental apparatus was developed to determine the pull-off force of a microparticles resting on one of the charged surfaces in an electrostatic particle dispenser. The resulting uncertainty in this force is approximately 12% at 95% confidence. Using this apparatus, the effects of humidity, pressure, temperature, particle composition, and surface roughness on the force required to remove the microparticle from a conducting surface can be quantified.

Preliminary studies conducted using this apparatus confirm the behavior described by proposed model (as given by Equation [4]). The pull-off force was determined to increase with increasing microparticle diameter and with increasing relative humidity. Further, values of the coefficients C_1, C_2, and C_3 obtained from these experiments are consistent with previous studies. Also, values of the surface energy determined from these measurements are comparable to within the uncertainty with published values.

Future experiments conducted using this apparatus will focus on detailed measurements to determine the precise effects of both relative humidity and surface roughness, as well as any possible correlation between the two effects. Further, studies investigating particles adhesion at forced "dry" conditions under vacuum are expected to yield insight into the mechanism behind the effect of relative humidity on particle adhesion by studying the efficiency with which the trapped water vapor can be removed by the low pressures over varying time periods. Finally, experiments focusing on alternate charging techniques are planned to study the feasibility of dispensing non-conducting particles using an electrostatic particle dispenser.

REFERENCES

Adamo, R. C., and Nanevicz, J. E. (1975). Parametric Study of Electrostatic Techniques for Aerosol Dispersion, *Stanford Research Inst*. Final Report:SRI Project, 3599.

Caylor, M. J., Dunn, P. F., and Brach, R. M. (1993). Low Velocity Impact of Electrically Charged Microspheres with Planar Surfaces under Vacuum Conditions, *J. Aerosol Sci*. 23.S1:S19–S22.

Cheng, W., Dunn, P. F., and Brach, R. M. (2002). Surface Roughness Effects on Microparticle Adhesion, *J. Adhesion*. 78:929–965.

Cho, A. W. H. (1964). Contact Charging of Micron–Sized Particles in Intense Electric Fields, *J. Appl. Phys*. 35.9:2561–2564.

Colver, G. M. (1976). Dynamic and Stationary Charging of Heavy Metallic and Dielectric Particles Against a Conducting wall in the Presence of a DC Applied Electric Field, *J. Appl. Phys*. 47.11:4839–4849.

Cooper, D. W., Wolfe, H. L., and Miller, R. J. (1988). In *Particles on Surfaces I: Detection, Adhesion, and Removal*. K. L. Mittal, ed. Plenum Press, New York, pp. 339–349.

Corn, M. (1961). The Adhesion of Solid Particles to Solid Surfaces, *J. Air Pollut. Contr. Assoc*. 11:566.

Derjaguin, B. V., Muller, V. M., and Toporov, Yu. P. (1975). Effect of Contact Deformations on the Adhesion of Particles. *J. Colloid and Interface Sci*. 53.2:314–326.

Dunn, P.F (2005). *Measurement and Data Analysis for Engineering and Science*. McGraw–Hill, New York.

Ibrahim, A., Dunn, P. F., and Brach, R. M. (2003). Microparticle Detachment from Surfaces Exposed to Turbulent Air Flow: Controlled Experiments and Modeling, *J. Aerosol Sci*. 34:765–782.

Ibrahim, A., Dunn, P. F., and Brach, R. M. (2004). Microparticle Detachment from Surfaces Exposed to Turbulent Air Flow: Effects of Flow and Particle Deposition Characteristics, *J. Aerosol Sci*. 35:805–821.

Johnson, K. L., Kendal, K., and Roberts, A. D. (1971). Surface Energy and the Contact of Elastic Solids, *Proc. R. Soc. Lond. A*. 324:301–313.

Maugis, D. (1991). Adhesion of Spheres: The JKR–DMT Transition Using a Dugdale Model, *J. Colloid and Interface Sci*. 150.1:243–269.

Myazdriker, O. A. and Pusanov, V. M. (1969). Instrument for Determining Adhesion Forces in a Surface Particle System, *Trans. from Zavodskaya Laboratoriya*. 25.10:1265–1267. Plenum, New York.

Novick, V. J., Hummer, C. R., and Dunn, P. F. (1989). Minimum DC electric Field Requirements for Removing Powder Layers from a Conductive Surface, *J. Appl. Phys*. 65.8:3242–3247.

Olansen, J. B., Dunn, P. F., and Novick, V. J. (1989). Dispensing Particles Under Atmospheric an Vacuum Conditions Using and Electrostatic Device, *J. Appl. Phys*. 66.12:6089–6109.

Osborne-Lee, I. W. (1988). Calculation of Hamaker Coefficients from Metallic Aerosols from Extensive Optical Data, in *Particles on Surfaces, Vol. 1*, K. L. Mittal, ed., Plenum, New York, 77–90.

Phares, D. J., Smedley, G. T., and Flagan, R. C. (2000). Effect of Particle Size and Material Properties on Aerodynamic Resuspension from Surfaces, *J. Aerosol Sci*. 31:1335–1354.

Shelton, H., Hendricks, Jr., C. D., and Wuerker, R. F. (1960). Electrostatic Acceleration of Microparticles to Hypervelocities, *J. Appl. Phys*. 31.7:1243–1246.

Visser, J. (1972). On Hamaker Constants: A Comparison Between Hamaker Constants and Lifshitz-Van der Waals Constants, *J. Advan. Colloid Interface Sci*. 31:331–363.